

Supplemental material

Belkaya et al., <https://doi.org/10.1084/jem.20190669>

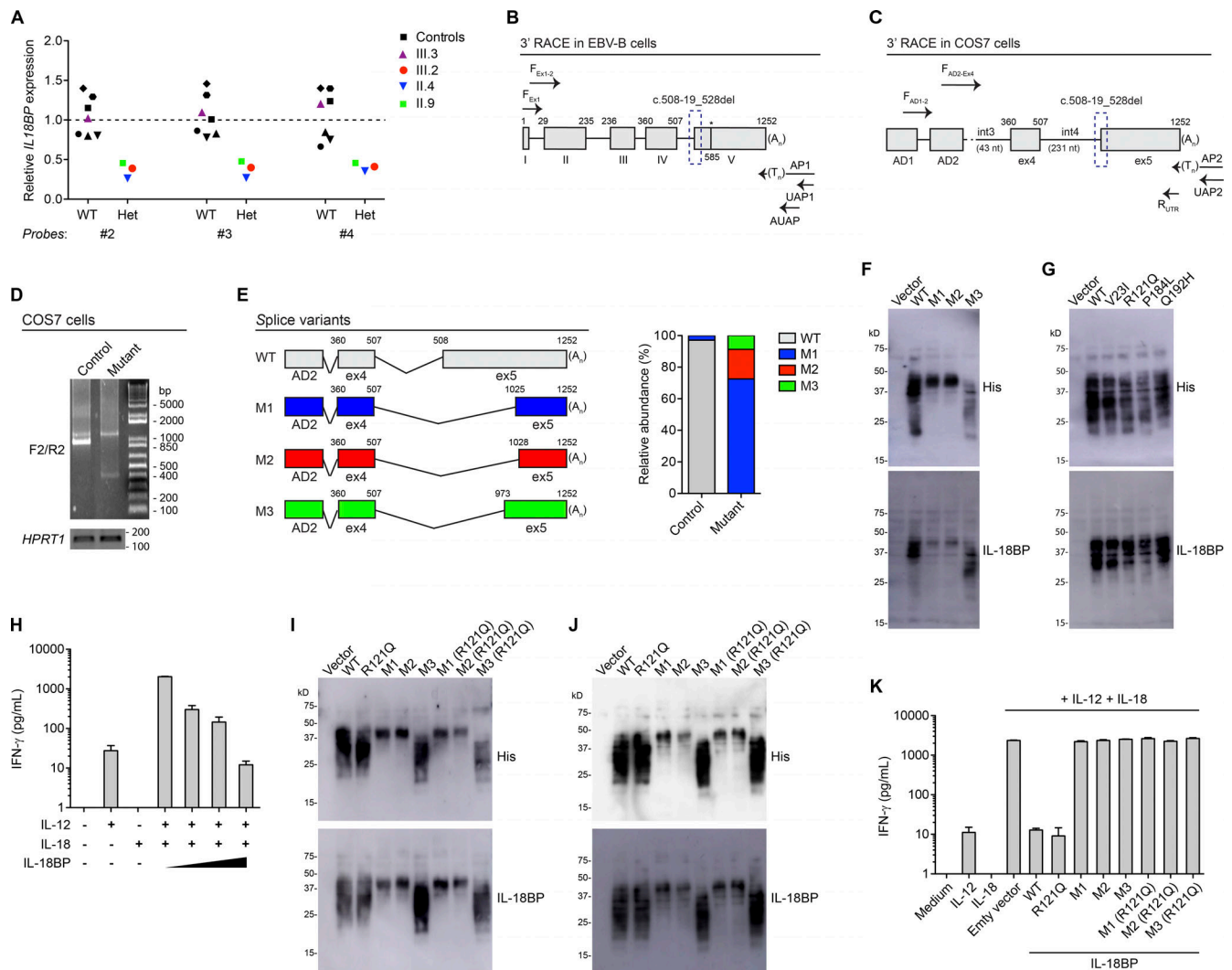
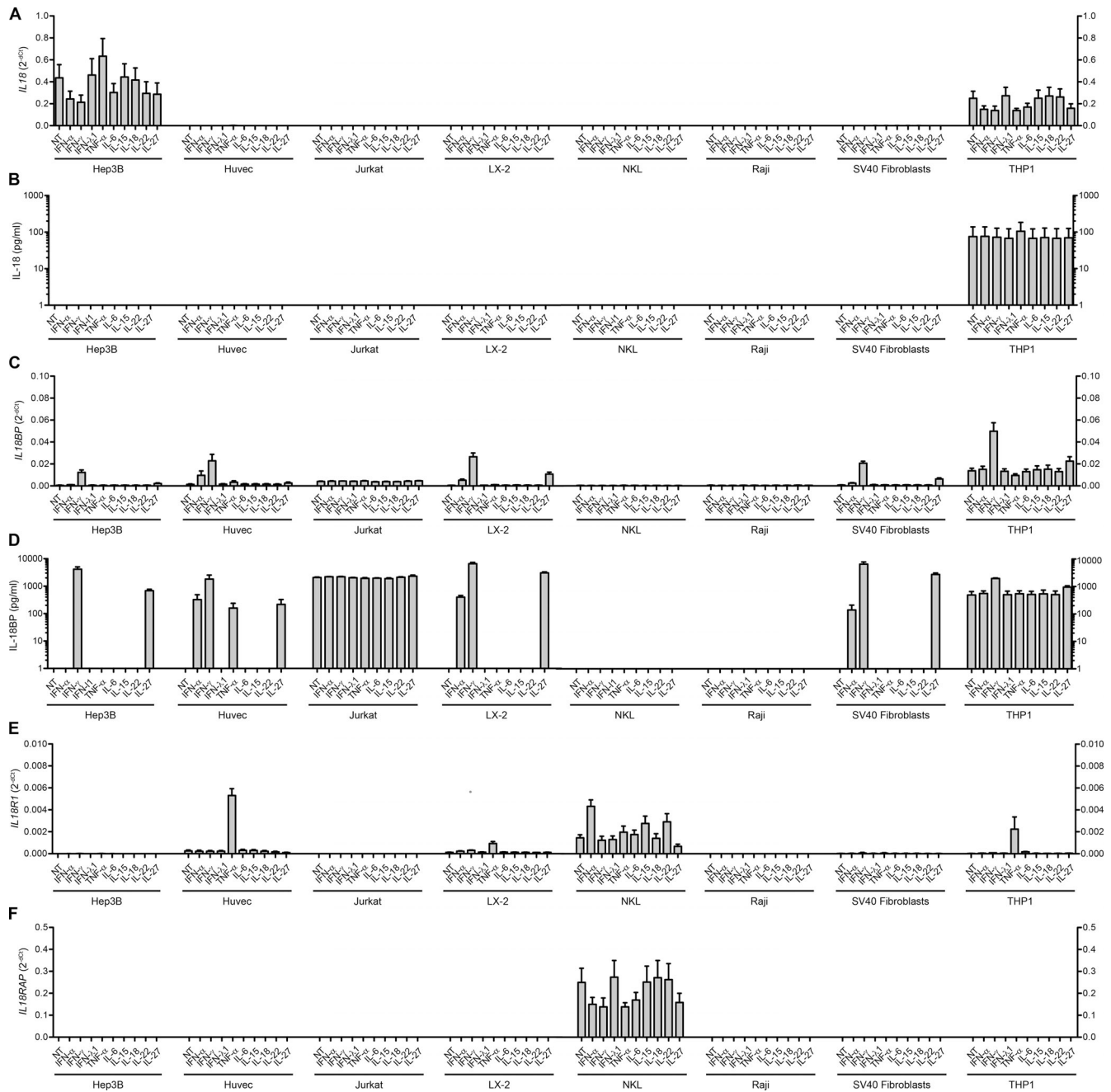


Figure S1. Impact of *IL18BP*:c.508-19_528del on gene expression and function. (A) RT-qPCR showing the level of *IL18BP* expression, assessed with various probes (Materials and methods), and normalized against endogenous *GAPDH*, in EBV-B cell lines from six healthy controls (black), the WT brother (III.3, purple), and heterozygous family members: brother (III.2, red), father (II.4, blue), and mother (II.9, green). Relative *IL18BP* expression was determined by normalization against the mean value for WT cells, which was set to 1 (indicated by a dashed line). The values shown are the means of two independent experiments performed in duplicate. (B and C) Diagrams showing the design for 3' RACE on *IL18BP* performed on EBV-B cell lines (B) or COS7 cells (C) using the pTAG4 3' exon-trapping vector. Numbers on the canonical *IL18BP* transcript begin with the start codon at position 1 and end with the polyadenylation site, indicated by A_n, at position 1,252. (D) Agarose gel electrophoresis showing aberrant splicing of *IL18BP* mRNA in 3' RACE on COS7 cells transfected with pTAG4 vectors carrying the WT or mutant *IL18BP* allele. *HPRT1* was used as the housekeeping gene control. (E) The nested PCR products from D were cloned, and colonies were sequenced. Diagram (left) and percentages (right) of WT (gray) and mutant (M1 in blue, M2 in red, and M3 in green) splice variants are shown. Clones with PCR artifacts or sequences that do not match with canonical *IL18BP* transcript were excluded from analyses. (F and G) Expression of WT and mutant IL-18BP isoforms (M1–M3) in F- and four missense variants (p.V23I, p.R121Q, p.P184L, and p.Q192H) from GnomAD in G, was assessed in the concentrated supernatants from transiently transfected COS7 cells with either empty vector or constructs expressing indicated IL-18BP variants. Immunoblotting was performed with the His tag antibody (top). The membrane was then stripped and probed with the IL18BP antibody (bottom). The concentrated supernatants were used in the IL-18BP bioassay experiments shown in Fig. 2 F. (H) IL-18BP bioassay: IFN- γ production was measured in NK-92 cells upon stimulation with recombinant human IL-12 (100 pg/ml), IL-18 (10 ng/ml), and/or IL-18BP at varying concentrations (0, 125, 250, or 500 ng/ml). Graph is presented on a logarithmic scale with base of 10. The data shown are means \pm SEM of two independent experiments performed in duplicate. (I and J) Expression of the mutant IL-18BP isoforms (M1–M3) carrying the common missense variant (p.R121Q) was assessed in the concentrated supernatants from transiently transfected COS7 cells with either empty vector or constructs expressing indicated IL-18BP variants. Two independent preparations are shown. Immunoblotting was performed with the His tag antibody (top). The membrane was then stripped and probed with the IL18BP antibody (bottom). (K) IL-18BP bioassay: IFN- γ production was measured in NK-92 cells after stimulation with recombinant human IL-12 (100 pg/ml), IL-18 (10 ng/ml), and/or concentrated supernatants (100 μ g/ml of total protein) of COS7 cells transiently transfected with either empty vector or the constructs expressing indicated IL-18BP variants. Graph is presented on a logarithmic scale with base of 10. The data shown are means \pm SEM of two independent experiments performed in duplicate using the supernatants shown in I and J.



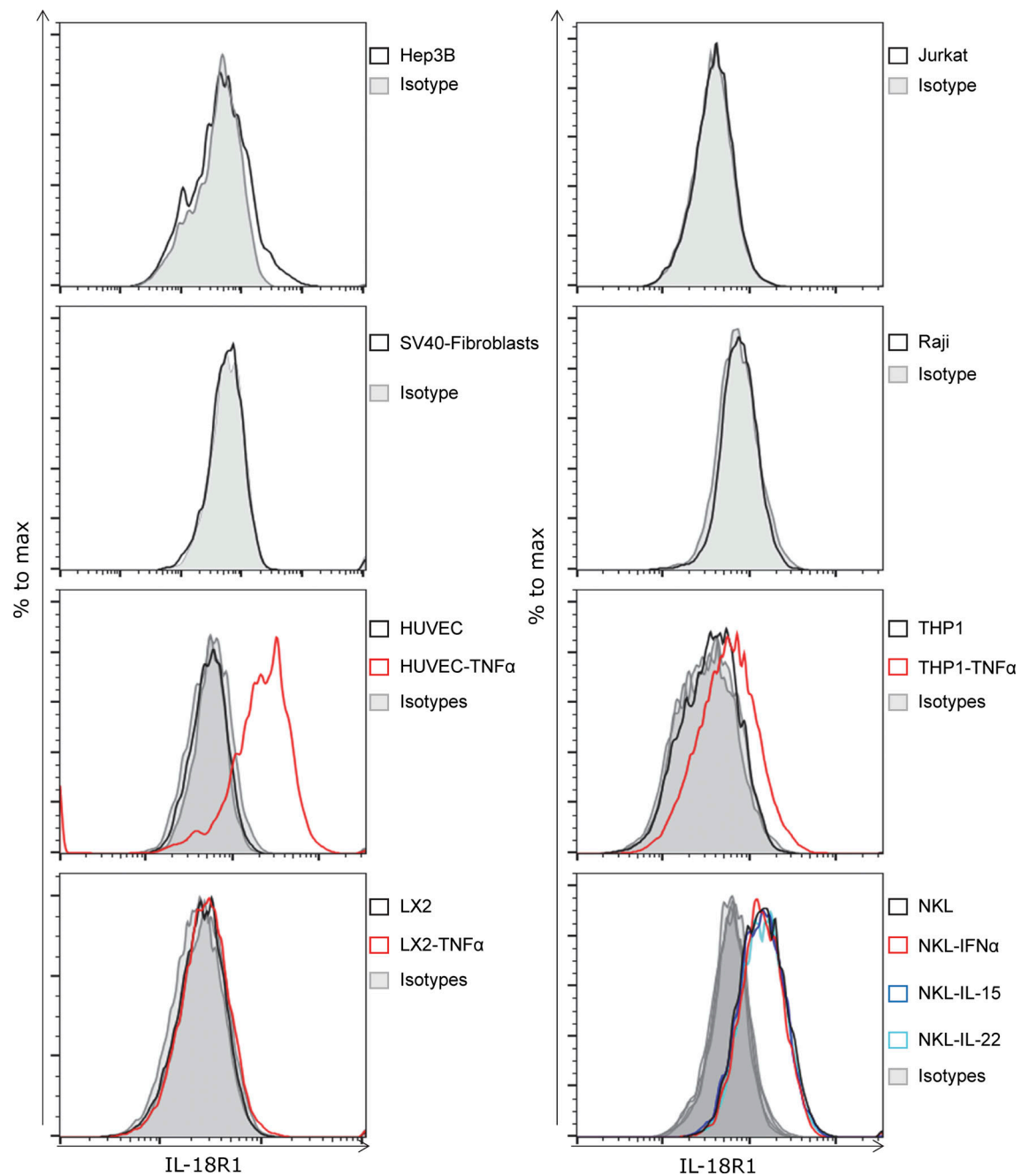


Figure S3. **Surface expression of IL-18R1 in various human cell lines.** Surface expression levels of IL-18R1 were assessed by flow cytometry on different human cell lines following stimulation with indicated inflammatory cytokines for 24 h.

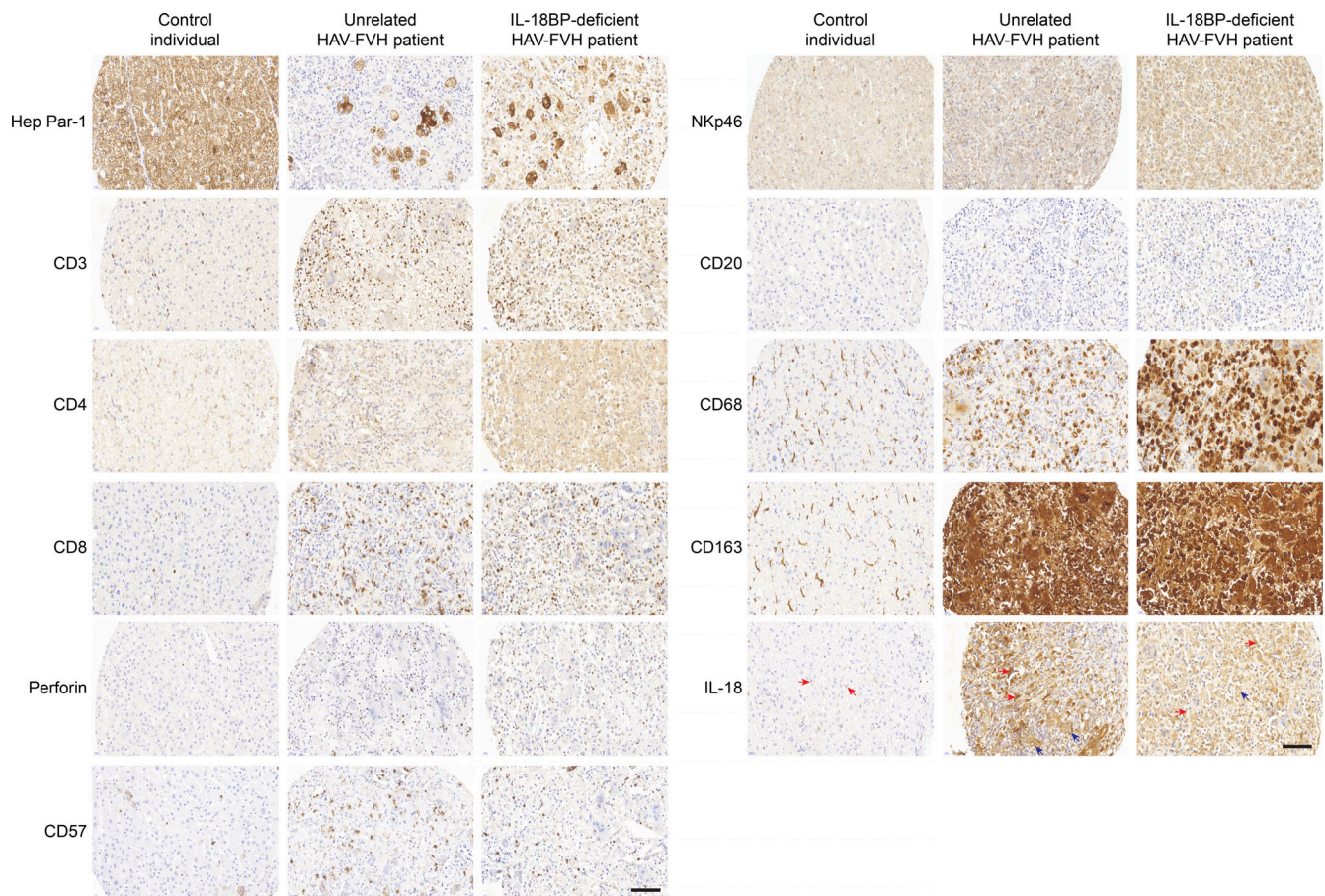


Figure S4. **Liver immunohistochemistry profile of patients with FVH.** Immunohistochemistry staining of liver tissue sections from a control individual, an unrelated patient with FVH due to HAV, and the deceased IL-18BP-deficient FVH patient reported in this study with the following markers: Hep Par-1, CD3, CD4, CD8, Perforin, CD57, NKp46, CD20, CD68, CD163, and IL-18. Hep Par-1 staining of the IL-18BP-deficient patient's liver tissue section displayed a background staining of macrophages, with lower intensity than hepatocytes. The IL-18BP-deficient patient and the unrelated FVH patient displayed also some residual hepatocytes positive for CD163 staining. Some IL-18-positive hepatocytes and macrophages are indicated with blue and red arrows, respectively. All images are shown at 400 \times magnification. Scale bars represent 100 μ m.

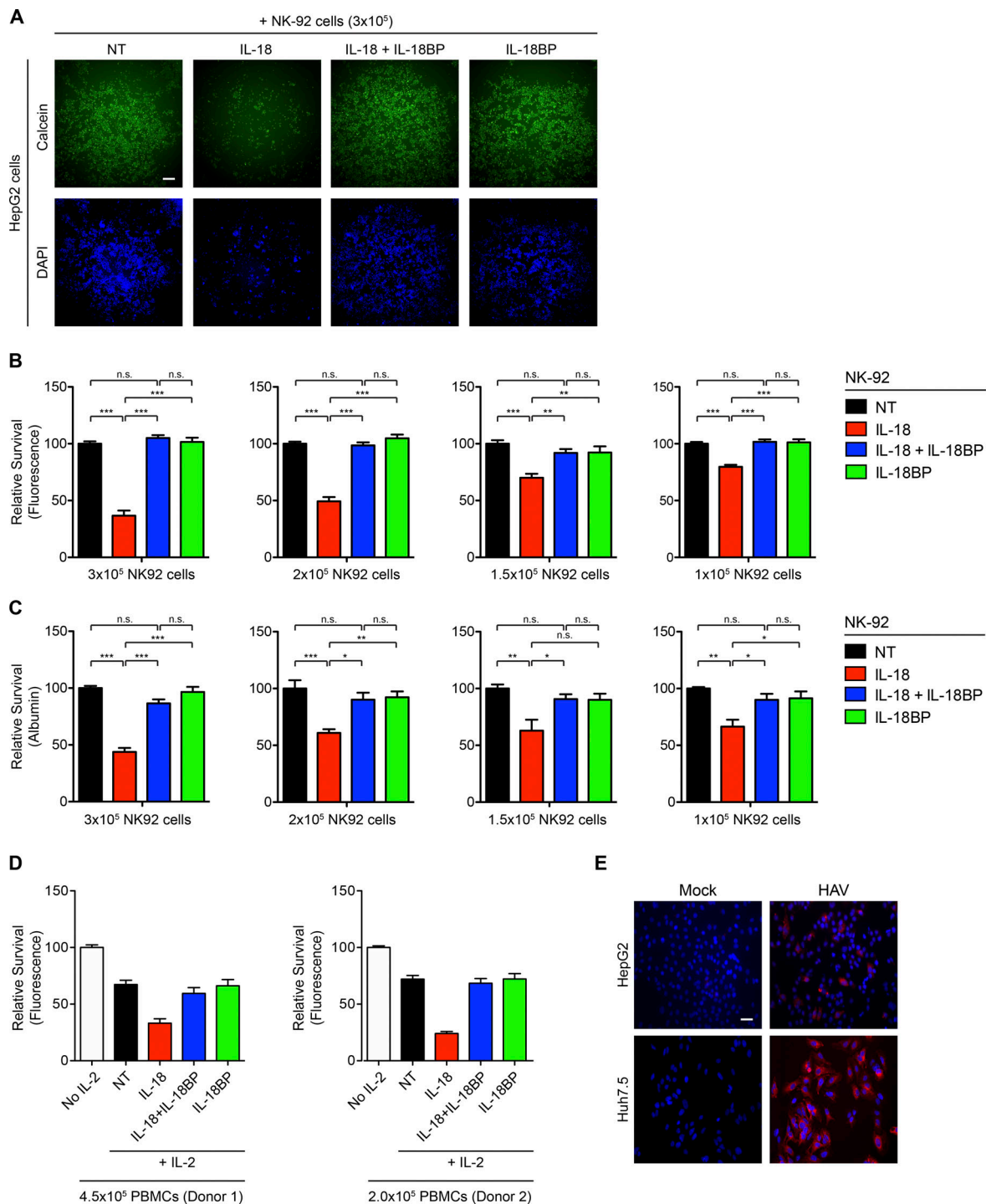


Figure S5. IL-18/IL-18BP-mediated hepatotoxicity. (A–C) Coculture of HepG2 cells and NK-92 cells either with no pretreatment (not treated [NT]) or pretreated with IL-18, IL-18 + IL-18BP, or IL-18BP. (A) Representative fluorescent images (4× magnification) are shown for IL-18/IL-18BP-mediated NK cell cytotoxicity against hepatocytes stained with Calcein-AM (green) and DAPI (blue). HepG2 cells were cultured with 3×10^5 NK cells per well. Scale bar represents 325 μ m. (B and C) IL-18/IL-18BP-mediated cytotoxicity against HepG2 cells shown for various numbers of NK-92 cells. The relative survival of HepG2 cells was calculated based on the measurement of fluorescence retention within cells (B) and the amount of secreted albumin (C). Relative fluorescence and albumin levels were determined by normalization against the mean value for HepG2 cells cocultured with NK92 cells without pretreatment (NT), set to 100. A decrease in the fluorescence or in albumin levels indicates an increase in NK cell-induced hepatotoxicity. Data are means \pm SEM of three independent experiments performed in quadruplicate for each group (n.s., not significant, *, $P < 0.05$; **, $P < 0.01$; ***, $P < 0.001$; one-way ANOVA with Bonferroni correction for multiple testing). (D) PBMCs isolated from two healthy individuals (donors 1 and 2) were pretreated with IL-18 and/or IL-18BP in the presence of IL-2 for 24 h and cultured with calcein-AM-stained HepG2 cells for 4 h. Relative fluorescence levels were determined by normalization against the mean value for HepG2 cells cocultured with PBMCs without IL-2 treatment, which was set to 100. Data are means \pm SEM of two independent experiments performed in quadruplicate. (E) Representative images show immunofluorescence staining for HAV infection in HepG2 and Huh7.5 cells at 20× magnification. Nucleus was stained with DAPI (blue). HAV-infected cells are in red. Scale bar represents 25 μ m.

Table S1. Genetic analysis of the WES data of the patient and two siblings

WES analysis	III.1 (Patient)	III.2 (Sibling)	III.3 (Sibling)
Total	142,213 (19,550)	141,383 (19,650)	141,145 (19,665)
Nonsynonymous and essential splicing	12,140 (6,148)	12,168 (6,232)	12,232 (6,234)
MAF <0.1%	241 (230)	240 (222)	271 (246)
Homozygous	9 (9)	12 (12)	7 (7)
Present only in the patient	6 (6)		

Data are presented as number of annotated variations with number of mutated genes shown in parentheses. Only nonsynonymous (indel-inframe, indel-frameshift, start-lost, missense, nonsense, stop-lost) and essential splice-site (splice acceptor and splice donor) variants were selected. Variants with an MAF of $\geq 0.1\%$ in public databases (EVS, 1000 Genomes, and GnomAD), including variants with an AF $\geq 0.1\%$ in each ethnic subpopulation (African, Ashkenazi Jewish, Finnish, non-Finnish European, South Asian, East Asian, and Latino) in GnomAD, were excluded. Finally, under the autosomal recessive model of inheritance, only homozygous variants were selected, and six genes with homozygous variants present only in the patient were considered to be candidate disease-causing genes.

Table S2. Homozygous rare nonsynonymous variations present only in the patient

Gene	GDI ^a	NI ^b	Variation		Zygosity			MAF	CADD/MS
			Type	Change	III.1	III.2	III.3		
<i>IL18BP</i>	2.05	1.764	Deletion	NM_173042.2:c.508-19_528del	hom	het	WT	0	28.2/12.19
<i>ADAMTS1</i>	4.70	0.100	Missense	NM_006988:p.Lys648Arg	hom	WT	WT	2.06×10^{-4}	25/17.33
<i>SLC6A19</i>	6.44	0.152	Missense	NM_001003841.2:p.Val551Met	hom	het	het	9.39×10^{-5}	25.1/14.87
<i>TM7SF2</i>	9.21	3.610	Missense	NM_003273.3:p.Ala36Gly	hom	het	WT	3.24×10^{-5}	16.63/16.48
<i>ZNF324</i>	1.65	0.143	Missense	NM_014347.2:p.Ile385Met	hom	het	het	0	23.2/12.19
<i>ZNF814</i>	2.16	0.005	Missense	NM_001144989.1:p.His407Asp	hom	het	het	3.54×10^{-5}	15.57/12.19

Six genes were identified with rare (MAF < 0.001) nonsynonymous variants present at homozygous state only in the patient. het, heterozygous; hom, homozygous; NI, McDonald-Kreitman neutrality index.

^aIn the GDI, the range is between 0.0001 for least-damaged human gene and 42.91 for most damaged human gene.

^bNI < 1 indicates a purifying selection.

Table S3. **Characteristics of genes with homozygous rare nonsynonymous variations present only in the patient**

Gene description	Expression pattern	Known function	Clinical significance
IL-18-binding protein (<i>IL18BP</i>)	Broad expression in spleen, appendix, lymph nodes, and 23 other tissues	Inhibitor of the proinflammatory cytokine IL18	Unknown
ADAM metalloproteinase with thrombospondin type 1 motif 1 (<i>ADAMTS1</i>)	Broad expression in ovary, placenta, and 17 other tissues	Role in growth, fertility, and organ morphology and function	Unknown
Solute carrier family 6 member 19 (<i>SLC6A19</i>)	Broad expression in small intestine, duodenum, and kidney	Transportation of most neutral amino acids across the apical membrane of epithelial cells	Biallelic mutations in this gene cause Hartnup disorder
Transmembrane 7 superfamily member 2 (<i>TM7SF2</i>)	Broad expression in adrenal, fat, and 20 other tissues	Role in cholesterol biosynthesis	Unknown
Zinc finger protein 324 (<i>ZNF324</i>)	Ubiquitous expression in brain, ovary, and 25 other tissues	May be involved in transcriptional regulation	Unknown
Zinc finger protein 814 (<i>ZNF814</i>)	Ubiquitous expression in prostate, spleen, and 25 other tissues	May be involved in transcriptional regulation	Unknown

Information related to the expression pattern, known function, and clinical significance of these six genes in humans were obtained from the NCBI Gene database.

Table S4. **Other clinical findings of the patient before FVH**

Clinical finding (reference value)	July 2004	October 2005	March 2007	October 2009	April 2011	September 2012	November 2013
Thyroiditis							
Anti-TPO (positive >60 IU/ml)	NA	Negative (<45)	Negative (<60)	NA	Positive (145)	NA	NA
Anti-PO (positive >10 IU/ml)	NA	NA	NA	Negative	Positive (51)	NA	NA
Anti-TG (positive >116 IU/ml)	NA	Negative (<90)	Negative (<60)	Positive	NA	NA	NA
Free T4 (normal, 1–1.07 ng/dl)	NA	NA	NA	NA	Positive (2.66)	Normalization upon treatment	
TSH (normal, 0.4–4 mIU/liter)	NA	NA	NA	NA	Positive (119.22)	Normalization upon treatment	
Celiac disease (excluded)							
RLA IgA anti-tTG (positive >150 cpm)	NA	Negative (<47)	Negative (<45)	Negative (<66)	NA	Negative (<44)	Negative (<129)
EMA	NA	Negative	Negative	Negative	NA	NA	NA
Langerhans anti-IC	Positive	NA	NA	NA	NA	NA	NA
Diabetes							
Anti-insulin (positive >0.7%)	Positive (1.31)	NA	NA	NA	NA	NA	NA
Anti-IA2 (positive >80 cpm)	Negative (<29)	NA	NA	NA	NA	NA	NA
Anti-GAD65 (positive >180 cpm)	Negative (<84)	NA	NA	NA	NA	NA	NA
Glycemia (normal, 4–6 mmol/liter)	High (37)	Normalization upon treatment					
HbA1c (normal, 4–5.6%)	High (8.9)	Normalization upon treatment					

EMA, endomysial antibodies (IgA); GAD65, glutamic acid decarboxylase; HbA1c, hemoglobin A1c; IA2, islet antigen 2; IC, islet cells; NA, not available; PO, peroxidase; RLA, radioligand receptor assay; T4, thyroxine; TG, thyroglobulin; TPO, thyroid peroxidase; TSH, thyroid-stimulating hormone; tTG, tissue transglutaminase.

Table S5. Analytical findings in the patient and siblings during the course of HAV infection

Finding (reference value)	Patient (III.1)					Sibling (III.2)					Sibling (III.3)					
	Day 1	Hospitalization				Hospitalization ^a			Day 5	Day 15	Hospitalization ^a			Day 4	Day 5	Day 15
		Day 8	Day 9 ^b	Day 10 ^c	Day 11 ^d	Day 1	Day 2	Day 3			Day 1	Day 2	Day 3			
IgM anti-HAV (IU/liter)	Positive (no value)	>60	ND	ND	ND	>60	ND	ND	ND	ND	>60	ND	ND	ND	ND	ND
ALT (<40 IU/liter)	2,181	1,481	1,117	275	403	42	35	29	27	23	1,594	1,298	894	757	531	96
AST (<40 IU/liter)	2,582	1,982	1,863	1,393	1,182	44	36	34	33	39	755	513	271	149	108	52
GGT (<25 IU/liter)	73	28	22	27	28	55	48	41	38	33	293	277	229	206	162	55
Factor V (>80%)	100	48	30	42	29	ND	ND	93	100	ND	100	ND	100	100	ND	ND
PT (>70%)	67	9	14	82	53	100	89	100	100	100	92	92	100	100	100	98

ND, no data.

^aTwo siblings (III.2 and III.3) were hospitalized 2 d after the patient died.

^bDay 9: Values were before liver transplantation.

^cDay 10: After transplantation values are shown.

^dDay 11: Patient died.

Table S6. Immunological phenotyping data of the patient during the course of HAV infection

PBMC (reference value)	Day 1	Day 8	Day 9	Day 10
Polymorphonuclear cells (normal, $1.5-8 \times 10^9$ /liter)	6.00	3.76	5.2	3.76
Lymphocytes (normal, $1.5-5 \times 10^9$ /liter)	2.21	1.44	2.26	2.38
Monocytes (normal, $0.1-1 \times 10^9$ /liter)	0.44	0.41	0.08	0.12

Table S7. List of primers used in this study

Name	Sequence (5'–3')	Application
Seq-1 Fwd	CAGCCTGTGAACTAATGCC	Sanger sequencing
Seq-1 Rev	GAATTTGGTGAGAGAAGGGA	Sanger sequencing
Seq-2 Fwd	CAAGGAGAGGCCTCCAG	Sanger sequencing
Seq-2 Rev	ACTCCAGGTAGACAGGTAG	Sanger sequencing
IL18BP SYBR Fwd ^a	CAGCTCTGGGCTGGGCTGAG	SYBR Green qPCR
IL18BP SYBR Rev ^a	GGGGTGTGTTGCGCATCCAC	SYBR Green qPCR
M1 SYBR Fwd	GGAACGTGGGAGCACAGGTA	SYBR Green qPCR
M1 SYBR Rev	TTGAGCGTTCCTGCCAGA	SYBR Green qPCR
M2 SYBR Fwd	GGAACGTGGGAGCACAGGTA	SYBR Green qPCR
M2 SYBR Rev	CTTGAGCGTTCCTCCAGAGC	SYBR Green qPCR
M3 SYBR Fwd	CCTGCACAGCACCAACTTCTC	SYBR Green qPCR
M3 SYBR Rev	GAGACATGGGAGTGGGAGCCA	SYBR Green qPCR
GAPDH SYBR Fwd ^b	GGAGCGAGATCCCTCCAAAT	SYBR Green qPCR
GAPDH SYBR Rev ^b	GGCTGTTGTCATACTTCTCATGG	SYBR Green qPCR
AP-1	CCAGTGAGCAGAGTGACGAGGACTCGAGCTCAAGCTTTTTTTTTTTTTTTT	Exon trapping
UAP-1	CCAGTGAGCAGAGTGACG	Exon trapping
AUAP	GAGGACTCGAGCTCAAGC	Exon trapping
F _{Ex1}	ATGACCATGAGACACAATGGA	Exon trapping
F _{Ex1-2}	CTGGACACCAGACCTCAGCC	Exon trapping/PCR
F _{Ex2-3}	CCACTGAATGGAACGCTGAG	PCR
R _{IL18BP_a}	TTAACCCTGCTGCTGTGGA	PCR
R _{IL18BP_b}	TCAAGTTGTGCTGCTGCT	PCR
R _{IL18BP_c}	TCACAGGCTGCTCTGGCA	PCR
pTAG4-IL18BP Fwd	CTGGAATTCCTTCTGCGCCTTCTCATG	Exon trapping
pTAG4-IL18BP Rev	GCACTCGAGGATGGATCTTTTCTAAATGTT	Exon trapping
AP-2	GCGGAATTCGGATCCCTCGAGTTTTTTTTTTTTTTTTTT	Exon trapping
UAP-2	GCGGAATTCGGATCCCTCGAGTT	Exon trapping
F _{AD1-2}	AGGGCCAGCTGTTGGGCTCG	Exon trapping
F _{AD2-Ex4}	CGTCGGCCTCCGAACCCGGGA	Exon trapping
R _{UTR}	CTCCATTGAATAATCCTTTATGAGGACC	Exon trapping
HPRT1 Fwd	CTGGCGTCGTGATTAGTGATGATG	Exon trapping
HPRT1 Rev	TTGAGCACACAGAGGGCTACAATG	Exon trapping
IL18BP BamHI (Kozak)	GTTGGATCCGCCACCATGAGACACAATGGACCA	Cloning
IL18BP-His XbaI	ATATCTAGATTAATGATGATGATGATGATGACCTGTGCTGGGACTGC	Cloning
V23I SDM Fwd	CTCCTGTGTGCCACATCGTCACTCTCCTGGTC	Mutagenesis
V23I SDM Rev	GACCAGGAGAGTGACGATGTGGGCACACAGGAG	Mutagenesis
R121Q SDM Fwd	AGGGGAGCACCAGCCAGGAACGTGGGAGCAC	Mutagenesis
R121Q SDM Rev	GTGCTCCACGTTCTGGCTGGTGTCTCCCT	Mutagenesis
P184L SDM Fwd	CACCCAAGAAGCCCTGCTCTCCAGCCACAG	Mutagenesis
P184L SDM Rev	CTGTGGCTGGAGAGCAGGGCTTCTTGGGTG	Mutagenesis
Q192H-His XbaI	ATATCTAGATTAATGATGATGATGATGATGACCTGATGCTGGGACTGC	Mutagenesis
M1-His XbaI	ATATCTAGATTAATGATGATGATGATGATGATGGGATGTTTTTTTTTTTTTTTCTCCATTGAATAATC	Cloning
M2-His XbaI	ATATCTAGATTAATGATGATGATGATGATGATGGGATGTTTTTTTTTTTTTTTCTCCATTGAATAATC	Cloning
M3-His XbaI	ATATCTAGATTAATGATGATGATGATGATGATGCTGAAGAGGCAGCATTCA	Cloning

Table S7. List of primers used in this study (Continued)

Name	Sequence (5'–3')	Application
M1 SDM Fwd	CCAGCTCTGGCAGGGGAACGCTCAAGCCTG	Mutagenesis
M1 SDM Rev	CGTTCCCCTGCCAGAGCTGGGCCAGGACGA	Mutagenesis
M2 SDM Fwd	CCAGCTCTGGGGGAACGCTCAAGCCTGGTT	Mutagenesis
M2 SDM Rev	GAGCGTTCCCCAGAGCTGGGCCAGGACGA	Mutagenesis
M3 SDM Fwd	CCAGCTCTGGCTCCCACTCCCATGTCTCTG	Mutagenesis
M3 SDM Rev	GGAGTGGGAGCCAGAGCTGGGCCAGGACGA	Mutagenesis

Fwd, forward; Rev, reverse.

^aKhalid et al., 2016.

^bPrimerBank ID: 378404907c1.

Reference

Khalid, K.E., H.N. Nsairat, and J.Z. Zhang. 2016. The presence of interleukin 18 binding protein isoforms in Chinese patients with rheumatoid arthritis. *AIMS Med. Sci.* 3:103–113. <https://doi.org/10.3934/medsci.2016.1.103>